

A Study on Thermal Behavior and Degradation kinetic of Microgels Based on PEG/Poly (NIPAM-co-AMPS)

Ajoy Kumar Saikia*

Department of Polymer Technology, Delhi Skill and Entrepreneurship University, Delhi, India

ABSTRACT

Temperature-responsive copolymeric microgels were synthesized via free radical polymerization of N-isopropylacrylamide (NIPAM) and acrylamido-2-methylpropyl sulphonic acid (AMPS) in presence of PEG as microinitiator under emulsifier free conditions. The thermal behavior of microgels in water was studied by dynamic light scattering (DLS) at different temperature. The temperature-dependent equilibrium constant derived from swelling data obtained from DLS and thermodynamic quantities are measured by Van't Hoff analysis. The thermogravimetric analysis was used for the evaluation of thermal stability and degradation kinetics of different microgel samples. The integral procedure decomposition temperature (IPDT) used to estimate the inherent thermal stability of microgels including volatile parts. The IPDT of microgel sample without AMPS was 368.99°C and the IPDT increased with increasing AMPS concentration in the feed composition. Thus, the thermal stability increased with increasing the AMPS concentration in the samples. The activation energy (E_a) of different microgel samples were calculated by using Broido and Horowitz & Metzger methods. The activation energy was found to be increases from 27.36 KJ/mol to 53.66 KJ/mol depending upon AMPS concentration in the feed composition. The glass transition temperature (T_g) of the microgel samples were examined by differential scanning calorimetric analysis. The stability and thermal degradation kinetics are important for designing copolymer blends in different area of applications.

Key words: Microgels, Thermal degradation, Kinetic parameters, Integral procedure, Decomposition temperature, Activation energy.

1. INTRODUCTION

Microgel particles are three-dimensional cross-linked polymeric network structures in the range of 50 nm to 5 μ m that swell in good solvents depending on the functional groups and cross-linking density. The swelling behavior of microgel particles is affected by many stimuli, including forces [1], temperature [2,3], pH [4,5] ionic concentration [6,7], and electric field [8,9].

Temperature responsive microgels are the most widely studied microgel particles among all stimuli. These microgels are being developed for diverse applications, such as drug delivery [10-20], biosensors [21-23], chemo-mechanical devices [24], separation/purification technologies [25], formation of responsive interfaces [26-29]. Textile [30], thin film and coating [31]. One of the most striking properties of temperature-sensitive poly (N-isopropylacrylamide) (PNIPAM) microgels is that they have the ability to undergo a reversible volume phase transitions temperature at $\sim 34.5^\circ\text{C}$ [32,33]. Below this temperature, the microgel particles are in a highly swollen state in the aqueous environment. However, when the temperature is raised above the VPTT, the polymer network collapses and expelling most of its water content along with any potentially dissolved molecule from the gel structure. The change in this phase transition is controlled by competing elastic, solvency, and ionic contributions.

The swelling properties of microgel particles are related to internal structure of individual particle. Wu *et al.*, [34] investigated the kinetics of particle formation and internal structure of PNIPAM particles. They found that during the particle formation the cross-linker monomer (NMBA) was incorporated into the microgel structure faster than

the N-isopropylacrylamide (NIPAM) monomer. This result implies that the different polymerization rates of the monomers lead to the formation of inhomogeneously cross-linked microgel particles. Hoare and Pelton [35] have also investigated how the functional group distribution (-COOH) affects the swelling of microgel particles. They found that microgel particles do not have a uniform distribution of comonomers within the particles, which in turn have an effect on the particle size distribution, swelling, stability, optical properties of microgels. It is well known that heat treatment of polymeric materials changes their morphological structure at temperatures higher than their glass transition temperature (T_g) which may lead to alter their electrical, optical, and thermal properties etc.

Thermal analysis is a very powerful technique to study the polymers structure [36]. To date, only differential scanning calorimetric (DSC) analysis was used to study the phase transition of PNIPAM hydrogels [37-39].

In this article, we are studying the phase transition using the Van't Hoff equation and thermal analysis study of copolymer microgels. Thermal

*Corresponding author:

E-mail: aksaikia2014@gmail.com

ISSN NO: 2320-0898 (p); 2320-0928 (e)

DOI: 10.22607/IJACS.2022.1001001

Received: 25th August 2021;

Revised: 25th December 2021;

Accepted: 02nd January 2022

gravimetric analysis (TGA) and DSC analysis were used for this study. The Broido and Horowitz-Metzger approximate methods are used to calculate the activation energies for comparison.

2. EXPERIMENTAL

2.1. Materials

The monomer NIPAM, acrylamido-2-methylpropyl sulphonic acid (AMPS) was purchased from Sigma-Aldrich and were used as received, PEG-6000 Merck Specialities Pvt. Ltd., Mumbai, N,N'-methylenebisacrylamide (MBA), ammonium ceric (IV) nitrate, 99.99% Sigma-Aldrich was dried in oven at 105°C for 1h prior to use, reagent grade nitric acid.

2.2. Preparation of Microgels

Polymerization was carried out in a round bottom flask connected to a water condenser, 1 g PEG was dissolved in 10 ml of distilled water to this solution 4 ml of 0.1 M $(\text{NH}_4)_2\text{Ce}(\text{NO}_3)_6$ solution prepared in 1N nitric acid was added and stirred for 5 min. Then the measured amount of NIPAM, acrylamido-2-methylpropyl sulphonic acid (AMPS) and MBA as cross-linker were added. Nitrogen was purged through the solution for 1 h to remove oxygen prior to polymerization. The polymerization was carried out at 50°C for 4 h under nitrogen atmosphere. The solution was then cooled to room temperature and then centrifuged 0.5 h (10,000 rpm, Eppendorf 5810R) at 40°C and then redispersed in distilled water. This process was repeated 3 times and then the samples were dried to a constant weight.

2.3. Characterization of Microgels

The hydrodynamic particle size and size distribution of microgel particles were measured at different temperature ranging from 25 to 50°C at constant copolymer concentrations in pure water by dynamic light scattering (DLS), Zetasizer Nano-S Malvern Instrument. The measurement was made at the scattering angle $\theta = 173^\circ$, wavelength (λ) = 633 nm. The time average scattering intensity correlation functions were obtained with an acquisition time of 30 S for each run. The results of size distribution were analyzed with a Laplace inversion program (CONTIN). Thermal degradation of gels was investigated by a thermogravimetric analyzer (Model Perkin Elmer, Pyris, Dimond TGA/DTA) from room temperature to 750°C with heating rate 10°C/min. under nitrogen atmosphere.

DSC measurements were performed on a TA instruments DSC Model 2010 in nitrogen atmosphere with 2–5 mg of polymer samples weighed in aluminum pans at a heating rate of 10°C/min.

3. RESULTS AND DISCUSSION

3.1. Thermal Behavior in Water

Thermo-responsive microgels were prepared by free-radical copolymerization of NIPAM and AMPS using PEG as macroinitiator in presence of MBA as cross-linking agent in water at 50°C. During the reaction PEG macroradicals were formed upon redox reaction of the $-\text{CH}_2\text{OH}$ end groups with Ce(IV) ($[\text{Ce}(\text{IV})]/[\text{OH end group}]$ 1.2/1) in acidic medium [30]. Macroradical initiates water-soluble AMPS, MBA, and NIPAM monomers which then grow in solution until they reach a critical chain length to become colloidal precursor particles. Either the precursor particles deposit onto an existing polymer particle or aggregate with other precursor particles until they form a particle sufficiently large to be colloidally stable. PEG also helps to increase the colloidal stability of precursor particle. These stable particles create nuclei for growing polymer chains, indicated by turning of clear reaction mixture into milky. The formation of particles through

precipitation polymerization mechanism is called soap-free emulsion polymerization. Due to the presence of negatively charged AMPS comonomer in the polymerization system, there is strong electrostatic repulsion among the sulfonate anion ($-\text{SO}_3^-$) which results in the expansion of network structure of microgels and have high water absorption properties.

The characterizations of particles size and particles size distribution of temperature-responsive microgels were investigated by means of DLS at different temperatures was reported in our previous article [40]. The swelling curves obtained show two-step process, where gel particles shift from swollen to collapsed state at temperature range 30–40°C as shown in Figure 1. The phase transition is an equilibrium process of the competing swollen and collapsed state. The equilibrium constant K_{eq} , which is equal to the ratio of (Collapsed)/(Swollen) [41] and determined from the swelling data of microgels. The cloud point measurement or DSC measurement done extensively used for the determination of phase transition of temperature of microgels [37–39]. Here, van't Hoff equation is used to measure ΔH , ΔS , ΔG of microgels sample from van't Hoff plot obtained by plotting $\ln K_{\text{eq}}$ versus $1/T$, which show two-stage process with different enthalpy, entropy component. The slope and intercept of the straight line give ΔH and ΔS , respectively, as shown in Figure 2.

The enthalpy for stage I is endothermic i.e 6.29 and 2.13 kJ/mol; entropy -6.53 and -5.32 J/mol K for MG-100 and MG-102 respectively. In stage I microgels show water swelling properties due to the formation of hydrogen bond between water molecules and amide groups of PNIPAM, PAMPS, and ionization of sulfonic acid group in PAMPS. At the transition temperature hydrogen bonding between the polymer and water molecules disrupted, result dehydration of the system, and water is released out of the polymer network with a large gain in entropy. The enthalpy for the Stage II is also endothermic, i.e., 12.18 and 26.01 kJ/mol; entropy value 4.26 and 5.45 J/mol K for MG-100 & MG-102, respectively. The enthalpy obtained in Stage II is comparable to water hydrogen bond $\Delta H \approx 10$ kJ/mol [42], thus; it assigned the loss of hydrogen bond above the transition temperature of polymer.

3.2. Thermal Stability

Thermogravimetric analysis is one of the common techniques to investigate the thermal stability and decomposition of different polymeric materials as a function of temperature or time [43]. Figure 3 shows the TGA thermograms of microgels with different concentrations

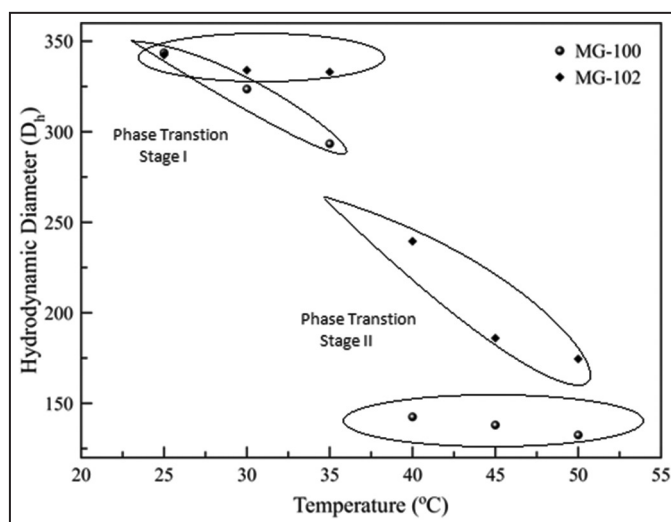


Figure 1: Hydrodynamic diameter of microgels at different temperature.

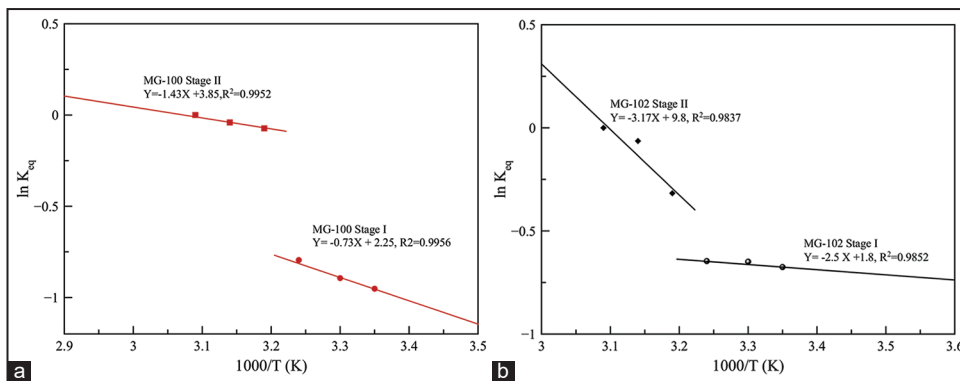


Figure 2: The van't Hoff plot for (a) MG-100, (b) MG-102.

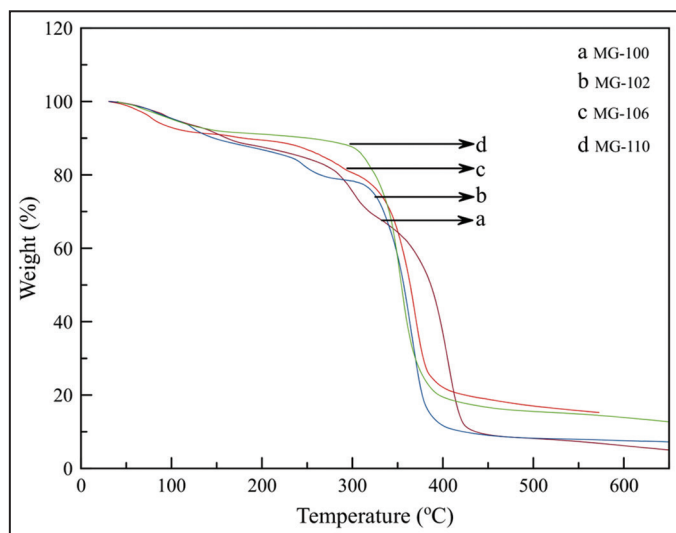


Figure 3: TGA thermograms of microgel samples with different AMPS content.

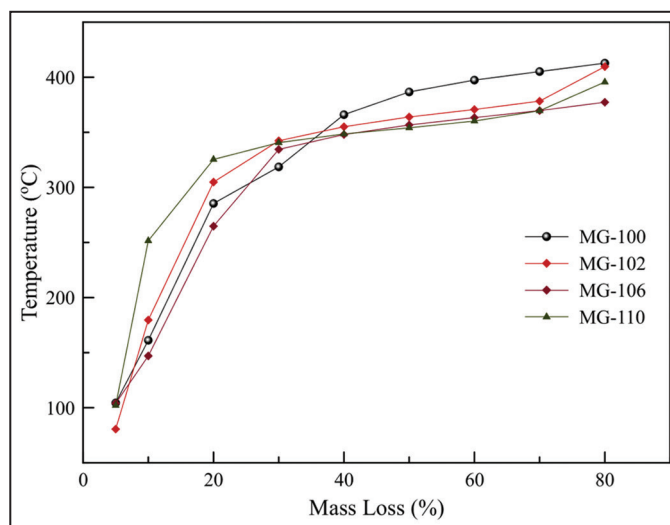


Figure 4: The weight loss temperature versus weight loss for microgel samples with different AMPS content.

of AMPS, from room temperature to 750°C in nitrogen atmosphere at heating rate 10°C/min and it observed that the rate of degradation of microgels slowed down with increasing AMPS concentration in the feed composition. Table 1 shows the characteristic temperature of thermal degradation of different microgels evaluated from TGA thermograms. It was observed that the microgels decomposed in two steps. The initial decomposition temperature of microgels samples increases from 39°C to 59°C whereas final decomposition temperature remains same for the sample MG-106 and MG-110. The weight loss involved in the first decomposition varied from 7 to 11% and in the second step of decomposition in ranged from 64 to 73%. All the microgel samples decomposed in the temperature range of 40–47°C. Figure 4 shows the weight loss temperature versus weight loss of microgel samples with different concentrations of AMPS. The thermal stability of sample MG-100 and MG-102 was lower than MG-106 and MG-110 and the weight loss % decreases with increasing AMPS concentration in the feed composition.

The integral procedure decomposition temperature (IPDT) which included the volatile parts of polymeric materials proposed by Doyle [44] and used to measure the inherent thermal stability of polymeric materials [45,46]. IPDT was calculated as per Doyle's method using the relation:

$$IPDT(°C) = A * K * (T_f - T_i) + T_i \tag{1}$$

$$A * = \frac{S_1 + S_2}{S_1 + S_2 + S_3} \tag{2}$$

$$K * = \frac{S_1 + S_2}{S_1} \tag{3}$$

Where A* is the area ratio of total experimental curve defined by the total TGA thermogram, T_i is the initial experimental temperature, T_f is the final experimental temperature. Figure 5 shows the representation of S₁, S₂, and S₃ for calculating A* and K*. The calculated results are given in Table 2, the IPDT of microgel samples found to be increase from 368.99 to 482.43°C with increasing the content of AMPS concentration. The incorporation of AMPS component improved the thermal stability of microgels by increasing the physical cross-linking or intermolecular hydrogen bonds between ether oxygen atoms in PEG chain and amide groups in microgels network.

The glass transition temperature (T_g) of the microgels was measured by DSC. Figure 6 presents the DSC thermogram of different microgels. The microgels sample MG-100 show a T_g at 114.5°C (ΔH 1.052 J/g; C_p 1398.8 mJ/°Cg) and MG-106 show at T_g at 144.96°C (ΔH 2.5 J/g; C_p 2320.69 mJ/°Cg). The glass transition temperature of microgel samples increases with increasing AMPS content in the samples. Glass transition temperature (T_g), enthalpy of transition (ΔH), and heat capacity (C_p) value obtained from DSC scans for different microgels are given in Table 2. The glass transition temperature depends on chain flexibility or mobility and polarity of polymeric materials, as the flexibility decreases when the glass transition temperature increased [47]. The incorporation of sulfonic acid makes the microgel structure more polar and rigid due to the inter or intramolecular force of interactions.

Table 1: Characteristic temperature for thermal degradation evaluated from TGA.

| Sample | Temperature Range for Step-I (°C) | Weight loss Step-I (%) | Temperature Range for Step-II (°C) | Weight loss Step-II (%) | Decomposition temperature Range (°C) | ΔT (°C) | IPDT ^a (°C) | IDT ^b (°C) |
|--------|-----------------------------------|------------------------|------------------------------------|-------------------------|--------------------------------------|---------|------------------------|-----------------------|
| MG-100 | 39–104 | 7 | 267–437 | 64 | 39–411 | 372 | 368.99 | 39 |
| MG-102 | 45–177 | 11 | 267–438 | 73 | 45–438 | 393 | 383.91 | 45 |
| MG-106 | 55–152 | 10 | 278–468 | 67 | 55–406 | 351 | 387.27 | 55 |
| MG-110 | 56–151 | 7 | 295–475 | 69 | 56–407 | 351 | 482.43 | 56 |

^aIntegral procedural decomposition temperature; ^bInitial decomposition temperature.

Table 2: Kinetic parameters for the decomposition of different Microgel samples.

| Sample | Stage | Temperature (°C) ^a | | T _g ^b (°C) | ΔH ^b (J/g) | C _p ^b mJ/°Cg | Activation energy, E _a (KJ/mol) | | R ² |
|--------|-------|-------------------------------|---------------------|----------------------------------|-----------------------|------------------------------------|--|------------------|----------------|
| | | Temperature range | Maximum temperature | | | | Broido | Horowitz-Metzger | |
| MG-100 | I | 39–104 | 104 | 114.5 | 1.052 | 1398.8 | 14.56 | 27.36 | 0.8779 |
| | II | 267–437 | 437 | | | | | | |
| MG-102 | I | 45–177 | 177 | 130.1 | 1.671 | 1594.2 | 16.66 | 46.06 | 0.9296 |
| | II | 267–438 | 438 | | | | | | |
| MG-106 | I | 55–152 | 152 | 144.9 | 2.5 | 2320.6 | 19.37 | 50.3 | 0.9566 |
| | II | 278–468 | 468 | | | | | | |
| MG-110 | I | 56–151 | 151 | 156.4 | 9.43 | 1749.6 | 24.65 | 53.66 | 0.8725 |
| | II | 295–475 | 475 | | | | | | |

^aFrom TGA thermograms, ^bFrom DSC thermograms.

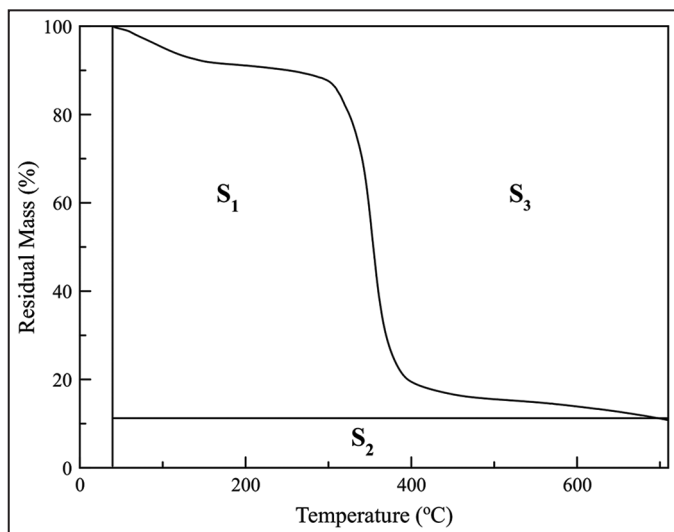


Figure 5: Schematic representation of S₁, S₂ and S₃ for A* and K*.

3.3. Kinetics of Thermal Degradation in Nitrogen Atmosphere

The degree of conversion (α) is defined as the ratio of the actual weight loss to the total weight loss.

$$\alpha = \frac{M_0 - M}{M_0 - M_\infty} \tag{4}$$

Where M is the actual weight at temperature T; M₀ is the initial weight and M_∞ is the weight at the end of non-isothermal experiments. The rate of degradation dα/dt, depends on the temperature and the weight of samples as given by equation-(1) [36].

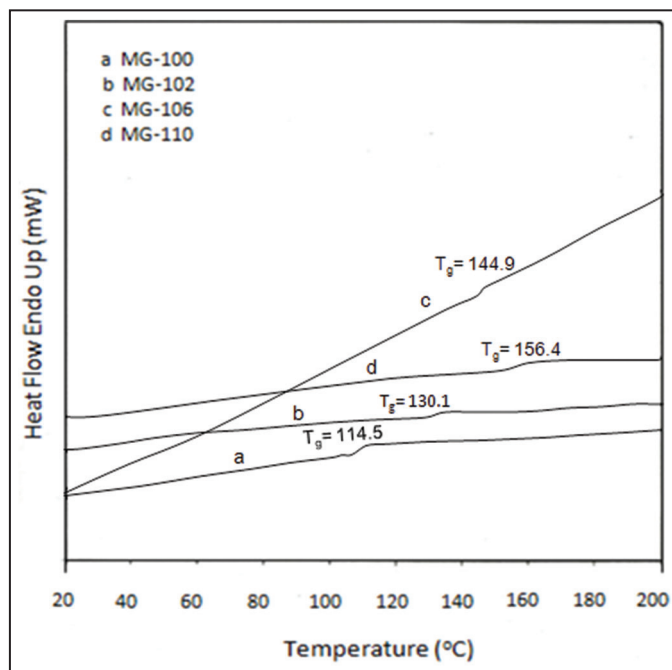


Figure 6: The DSC thermograms of different microgel samples.

$$\frac{d\alpha}{dt} = k(T)f(\alpha) \tag{5}$$

Where k(T) is the rate constant and f(α) is a function of conversion.

If k(T)=A exp^(-Ea/RT) and f(α)=(1-α)ⁿ then equation-(1) can be expressed as:

$$\frac{d\alpha}{dt} = A \exp^{(-Ea/RT)} (1 - \alpha)^n \tag{6}$$

Where A represents the pre-exponential factor; E_a is the activation energy; R is the gas constant; T is the absolute temperature and n is the reaction order.

$$\frac{d\alpha}{(1-\alpha)^n} = \left[\frac{A \exp(-E_a/RT)}{\beta} \right] dT \quad (7)$$

Where β is the rate of heating, A large number of pyrolysis process is represented with as first-order reaction [48]. Therefore, we assume $n = 1$ for further calculation. Integrating the equation-(4), we get

$$\ln(1-\alpha) = -\frac{A}{\beta} \int_{T_0}^{T_1} \exp(-E_a/RT) dT \quad (8)$$

The integration of equation-(8) is used to calculate the Horowitz and Metzger approximate.

$$\ln(1-\alpha) = -\frac{ART_m^2}{\beta E_a} \exp\left[\frac{-E_a(1-\theta/T_m)}{RT_m}\right] \quad (9)$$

Where $\theta = T - T_m$, T_m is the temperature of maximum degradation rates, when $T = T_m$, $\theta = 0$ and $\ln(1-\alpha) = -1$, the equation-(6) becomes

$$-1 = -\frac{ART_m^2}{\beta E_a} \exp[-E_a / RT_m] \quad (10)$$

The substitution of this equation in equation-(9), we get

$$\ln(1-\alpha) = -\exp\left(\frac{E_a \theta}{RT_m^2}\right) \text{ or}$$

$$\ln(-\ln(1-\alpha)) = \frac{E_a \theta}{RT_m^2}$$

Thus, the plot of $\ln(-\ln(1-\alpha))$ versus θ gives a straight line whose slope is E_a / RT_m^2 , and this procedure to calculate the activation energy is called the Horowitz-Metzger method [49].

In the Broido method, $\exp(-E_a/RT) \cong (T_m/T)^n \exp(-E_a/RT)$, The temperature range of analysis is close to T_m [48]³⁶. The equation-(5) may be written as

$$\ln(1-\alpha) = -\frac{ART_m^2}{\beta E_a} \exp(-E_a / RT)$$

Or

$$\ln(-\ln(1-\alpha)) = -\frac{E_a}{RT} + \text{constant}$$

By plotting $\ln(-\ln(1-\alpha))$ versus $1/T$ gives the straight line with slope $-E_a/R$, the activation energy is calculated from the slope. Figures 7 and 8 show the application of Broido and Horowitz-Metzger method for different samples. The activation energy obtained by both the Broido and Horowitz-Metzger methods are presented in Table 2. The difference in the values of the activation energy observed when it compared for the same composition of the samples. The different values of activation energy obtained are due to calculation method for a particular composition of microgel samples, i.e., activation energy calculated by Horowitz & Metzger method gives higher values. The activation energy calculated by both methods increased with increasing the AMPS content in the feed composition. This indicates that when

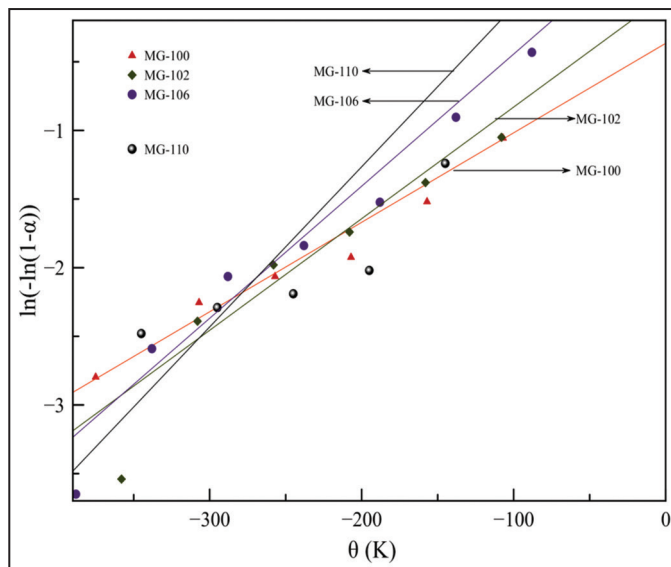


Figure 7: $\ln[-\ln(1-\alpha)]$ versus θ plots using Horowitz-Metzger method for the Microgel samples.

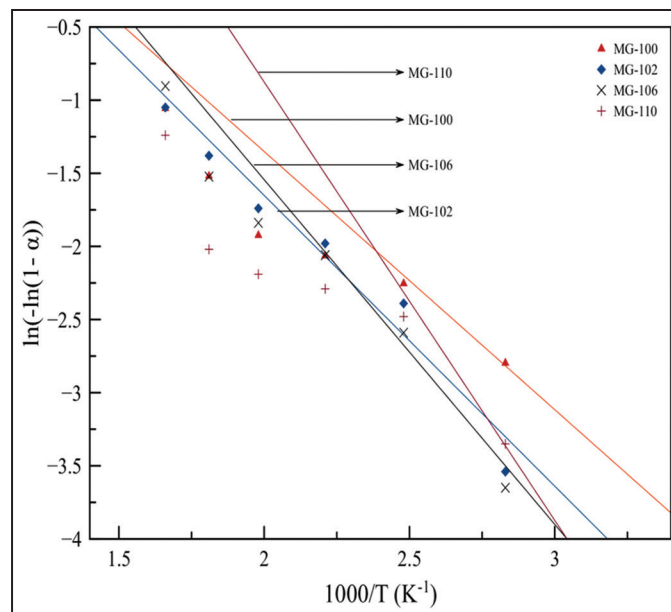


Figure 8: $\ln[-\ln(1-\alpha)]$ versus $1/T$ plots using Broido method for the Microgel samples.

energy barrier increases the weight loss process becomes more stable at higher temperature in respect to the composition of AMPS. The degradation of microgel samples depends on AMPS concentration with distinct activation energies from 27.36 KJ/mol to 53.66 KJ/mol.

4. CONCLUSION

Temperature-sensitive microgels with different compositions were prepared by soap-free emulsion polymerization. The composition of the microgels was controlled by adjusting the monomer feed composition and investigated the influence of the AMPS monomer concentration on phase transition behavior, thermal stability, and kinetics of thermal degradation for the different microgel samples. The thermal stability of microgel samples was improved by incorporation of AMPS monomer, thus it reduce the possibilities of physical changes during the processing and service condition. The activation energies (E_a) for all

the microgel samples increase with increasing AMPS concentration in the feed composition which is an indication of relative thermal stability of the microgels. Both Broido and Horowitz-Metzger methods give the different calculation results of activation energies. The variations of the calculated values may be due to the approximation used to evaluate the respective kinetic equations.

5. ACKNOWLEDGMENT

The author sincerely thank to Dr. Jitu Ranjan Chetia, Department of Chemistry, Dibrugarh University, Assam, India for his generous help with operating TGA/DTA, DSC instrument and helpful discussion.

6. REFERENCES

1. M. Doi, (2009) Gel dynamics, *Journal of Physical Society of Japan*, **78**: 052001.
2. C. Cheng, M. Schmidt, A. Zhang, A. D. Schluter, (2007) Synthesis of Thermally Switchable Poly(*N*-isopropylacrylamide-*block*-dendronized methacrylate)s, *Macromolecules*, **40**: 220-227.
3. A. K. Saikia, U. K. Mandal, S. Aggarwal, (2012) Network structure and temperature dependence swelling behavior of PEG-*b*-Poly (NIPAM-co-AMPSA) hydrogels in water, *Journal Polymer Research*, **19**: 9871.
4. R. Marcombe, S. Q. Cai, W. Hong, X. H. Zhao, Y. Lapusta, Z. G. Suo, (2010) A theory of constrained swelling of a pH-sensitive hydrogel, *Soft Matter*, **6**: 784-793.
5. E. Turan, S. Demirci, T. Caykara, (2008) Thermo- and pH-induced phase transitions and network parameters of poly (N-isopropylacrylamide-co-2-acrylamido-2-methylpropanosulfonic acid) hydrogels, *Journal of Applied Polymer Science Part B: Polymer Physics*, **46**: 1713-1724.
6. K. van Durme, H. Rahier, B. van Mele, (2005) Influence of additives on the thermoresponsive behavior of polymers in aqueous solution, *Macromolecules*, **38**: 10155-10163.
7. S. I. Yusa, K. Fukuda, T. Yamamoto, Y. Iwasaki, A. Watanabe, K. Akiyoshi, Y. Morishima, (2007) Salt effect on the heat-induced association behavior of gold nanoparticles coated with poly (N-isopropylacrylamide) prepared via reversible addition-fragmentation chain transfer (RAFT) radical polymerization, *Langmuir*, **23**: 12842-12848.
8. Y. Osada, J. P. Gong, (1998) Soft and wet materials: Polymer gels, *Advanced Materials*, **10(11)**: 827-837.
9. T. Shiga, (1997) Deformation and viscoelastic behavior of polymer gels in electric fields, *Advances in Polymer Science*, **134**: 131-163.
10. A. K. Saikia, S. Aggarwal, U. K. Mandal, (2013) Preparation and controlled drug release characteristics of thermoresponsive PEG/poly (NIPAM-co-AMPS) hydrogels, *International Journal of Polymeric Materials and Polymeric Biomaterials*, **62(1)**: 39-44.
11. G. H. Hsiue, S. H. Hsu, C. C. Yang, S. H. Lee, I. K. Yang, (2002) Preparation of controlled release ophthalmic drops, for glaucoma therapy using thermosensitive poly-N-isopropylacrylamide, *Biomaterials*, **23**: 457-462.
12. S. H. Choi, J. J. Yoon, T. G. Park, (2002) Galactosylated poly (N-isopropylacrylamide) hydrogel submicrometer particles for specific cellular uptake within hepatocytes, *Journal Colloid Interface Science*, **251**: 57-63.
13. N. Murthy, Y. X. Thng, S. Schuck, M. C. Xu, J. M. J. Frechet, (2002) A novel strategy for encapsulation and release of proteins: Hydrogels and microgels with acid-labile acetal cross-linkers, *Journal of American Chemical Society*, **124**: 12398-12399.
14. V. C. Lopez, M. Snowden, (2003) The role of colloidal microgels in drug delivery, *Journal of Drug Delivery System and Science*, **3**: 19-23.
15. S. Nayak, H. Lee, J. Chmielewski, L. A. Lyon, (2004) Folate-mediated cell targeting and cytotoxicity using thermoresponsive microgels, *Journal of American Chemical Society*, **126**: 10258-10259.
16. C. M. Nolan, C. D. Reyes, J. D. Debord, A. J. Garcia, L. A. Lyon, (2005) Phase transition behavior, protein adsorption, and cell adhesion resistance of poly (ethylene glycol) cross-linked microgel particles, *Biomacromolecules*, **6**: 2032-2039.
17. M. V. Varma, A. M. Kaushal, S. Garg, (2005) Influence of micro-environmental pH on the gel layer behavior and release of a basic drug from various hydrophilic matrices, *Journal of Controlled Release*, **103**: 499-510.
18. V. C. Lopez, J. Hadgraft, M. J. Snowden, (2005) The use of colloidal microgels as a transdermal drug delivery system, *International Journal Pharmaceutics*, **292**: 137-147.
19. C. M. Nolan, L. T. Gelbaum, A. L. Lyon, (2006) ¹H NMR investigation of thermally triggered insulin release from poly (N-isopropylacrylamide) microgels, *Biomacromolecules*, **7**: 2918-2922.
20. T. R. Hoare, D. S. Kohane, (2008) Hydrogels in drug delivery: Progress and challenges, *Polymer*, **49**: 1993-2007.
21. G. E. Morris, B. Vincent, M. J. Snowden, (1997) The interaction of thermosensitive, anionic microgels with metal ion solution species, *Progress in Colloid Polymer Science*, **105**: 16-22.
22. J. R. Retama, B. Lopez-Ruiz, E. Lopez-Cabarcos, (2003) Microstructural modifications induced by the entrapped glucose oxidase in cross-linked polyacrylamide microgels used as glucose sensors, *Biomaterials*, **24**: 2965-2973.
23. Z. Guo, H. Sautereau, D. E. Kranbuehl, (2005) Structural evolution and heterogeneities studied by frequency-dependent dielectric sensing in a styrene/dimethacrylate network, *Macromolecules*, **38**: 7992-7999.
24. I. Varga, I. Szalai, R. Meszaros, T. Gilanyi, (2006) pH-responsive nanogels, *Journal of Physical Chemistry B*, **110(41)**: 20297-20301.
25. L. Bromberg, M. Temchenko, T. A. Hatton, (2003) Smart microgel studies. Polyelectrolyte and drug-absorbing properties of microgels from polyether-modified poly (acrylic acid), *Langmuir*, **19(21)**: 8675-8684.
26. V. Nerapusri, J. L. Keddie, B. Vincent, I. A. Bushnak, (2008) Absorption of cetylpyridinium chloride into poly (N-isopropylacrylamide)-based microgel particles, in dispersion and as surface-deposited monolayers, *Langmuir*, **23(19)**: 9572-9577.
27. S. Schmidt, T. Hellweg, R. von Klitzing, (2008) Packing density control in poly (NIPAM-co-AAc) microgel monolayers: Effect of surface charge, pH, and preparation technique, *Langmuir*, **24(21)**: 12595-12602.
28. M. J. Serpe, C. D. Jones, L. A. Lyon, (2003) Layer-by-layer deposition of thermoresponsive microgel thin films, *Langmuir*, **19(21)**: 8759-8764.
29. R. Acciaro, C. Aulin, L. Wagberg, T. Lindstrom, P. M. Claesson, I. Varga, (2011) Investigation of the formation, structure and release characteristics of self-assembled composite films of cellulose nanofibrils and temperature responsive microgels, *Soft Matter*, **7(4)**: 1369-1377.
30. M. D. C. Topp, H. Leunen, P. J. Dijkstra, K. Tauer, C.

- Schellenberg, J. Feijen, (2005) Quasi-living polymerization of N-isopropylacrylamide onto poly (ethylene glycol), *Macromolecules*, **33(14)**: 4986-4988.
31. R. M. P. da Silva, J. F. Mano, R. L. Reis, (2007) Smart thermoresponsive coatings and surfaces for tissue engineering: Switching cell-material boundaries, *Trends in Biotechnology*, **25(12)**: 577-583.
32. T. Hirokawa, T. Tanaka, (1984) Volume phase transition in a nonionic gel, *Journal of Chemical Physics*, **81(12)**: 6379-6388.
33. H. Kawasaki, S. Sasaki, H. Maeda, (1998) Effects of the gel size on the volume phase transition of poly (N-isopropylacrylamide) gels: A calorimetric study, *Langmuir*, **14(4)**: 773-776.
34. X. Wu, R. H. Pelton, A. E. Hamielec, D. R. Woods, W. McPhee, (1994) The kinetics of poly(N-isopropylacrylamide) microgel latex formation, *Colloid and Polymer Science*, **272**: 467-477.
35. T. Hoare, R. Pelton, (2007) Functionalized microgel swelling: Comparing theory and experiment, *Journal of Physical Chemistry B*, **111(41)**: 11895-11906.
36. T. Hatakeyama, F. X. Quinn, (1994) *Thermal Analysis: Fundamentals and Application to Polymer Science*, New York, United States: Johan Wiley & Sons.
37. Y. Weng, Y. Ding, G. Zhang, (2006) Microcalorimetric investigation on the lower critical solution temperature behavior of N-isopropylacrylamide-co-acrylic acid copolymer in aqueous solution, *Journal of Physical Chemistry B*, **110(24)**: 11813-11817.
38. N. C. Woodward, B. Z. Chowdhry, M. J. Snowden, S. A. Leharne, P. C. Griffiths, A. L. Winnington, (2003) Calorimetric investigation of the influence of cross-linker concentration on the volume phase transition of poly (N-isopropylacrylamide) colloidal microgels, *Langmuir*, **19(8)**: 3202-3211.
39. M. Anderson, S. L. Maunu, (2006) Volume phase transition and structure of poly (N-isopropylacrylamide) microgels studied with ^1H -NMR spectroscopy in D_2O , *Colloid and Polymer Science*, **285**: 293-303.
40. A. K. Saikia, U. K. Mandal, S. Aggarwal, (2013) Swelling dynamics of poly (NIPAM-co-AMPS) hydrogels synthesized using PEG as macroinitiator: Effect of AMPS content, *Journal of Polymer Research*, **20**: 31.
41. C. V. Rice, (2006) Phase-transition thermodynamics of N-isopropylacrylamide hydrogels, *Biomacromolecules*, **7(10)**: 2923-2925.
42. W. J. Moore, (1972) *Physical Chemistry*, Hyderabad: Orient Longman Ltd.
43. S. Vyazovkin, (2000) Kinetic concepts of thermally stimulated reactions in solids: A view from a historical perspective, *International Reviews in Physical Chemistry*, **19(1)**: 45-60.
44. C. D. Doyle, (1961) Estimating thermal stability of experimental polymers by empirical thermogravimetric analysis, *Analytical Chemistry*, **33(1)**: 77-79.
45. S. J. Park, H. C. Kim, H. I. Lee, D. H. Suh, (2001) Thermal stability of imidized epoxy blends initiated by N-benzylpyrazinium hexafluoroantimonate salt, *Macromolecules*, **34(22)**: 7573-7575.
46. C. L. Chiang, R. C. Chang, Y. C. Chiu, (2007) Thermal stability and degradation kinetics of novel organic/inorganic epoxy hybrid containing nitrogen/silicon/phosphorus by sol-gel method, *Thermochimica Acta*, **453(2)**: 97-104.
47. L. Ma, L. Zhang, J. C. Yang, X. M. Xie, (2002) Improvement in the water-absorbing properties of superabsorbent polymers (acrylic acid-co-acrylamide) in supercritical CO_2 , *Journal of Applied Polymer Science*, **86(9)**: 2272-2278.
48. A. Broido, (1969) A simple, sensitive graphical method of treating thermogravimetric analysis data, *Journal of Polymer Science Part A-2: Polymer Physics*, **7**: 1761-1773.
49. H. W. Horowitz, G. Metzger, (1963) A new analysis of thermogravimetric traces, *Analytical Chemistry*, **35(10)**: 1464-1468.

*Bibliographical Sketch



Dr. Ajoy Kumar Saikia work as Assistant Professor in Department of Polymer Technology, Delhi Skill and Entrepreneurship University, GND DSEU Rohini Campus, Delhi, has more than 20 years of teaching experience. During his tenure he has made significant contribution towards institutional development by performing duties in various capacities at the administrative level. His research interest include Smart polymers, Bio/Nanocomposites, designing of drug delivery system. His research concentrated on understanding several important scientific and technological aspects based on Nano Science and technology especially in the designing and development of smart polymers, hybrid nanomaterials for biomedical applications. He has published a number of research papers in international reputed peer reviewed Journals; delivered talks in different national and international conferences; and been a reviewer of various international peer reviewed journals.